

Basalt Melting by Localized-Microwave Thermal-Runaway Instability

E. Jerby*, Y. Meir, M. Faran

Tel Aviv University, Ramat Aviv 69978, Israel

* E-mail: jerby@eng.tau.ac.il

This paper presents an experimental and theoretical study of the thermal-runaway instability induced by localized microwaves in basalt stones. This effect leads to the inner melting of the basalt core, and further to its eruption similarly to a volcanic burst. The experiments are conducted in a single-mode cavity at 2.45 GHz, 0.9 kW. The microwave-induced miniature volcano exhibits hotspots, bursts and eruption of lava, and solidification of lava flows to volcanic glass (obsidian), similarly to real volcanic phenomena. The numerical simulation, taking into account the temperature dependence of the basalt properties, is compared to the experimental measurements. The results may lead to the development of new means for mining and construction in basalt, as well as for demonstrating volcanic phenomena in laboratories, schools and museums.

Keywords: Basalt, Melting, Microwaves, Thermal-runaway, Localized heating

INTRODUCTION

Basalts, the most common volcanic rocks on earth, appear in nature in a range of physical and chemical properties, and a variety of outer shapes [1]. Mining and construction operations in basalt are of a great interest, hence the development of new tools such as the microwave drill [2] may advance the effectiveness of these operations in several scenarios. In another aspect, volcanoes and related geophysical phenomena have a great environmental importance. These are studied mainly by field observations and measurements, and by theoretical models and numerical studies, hence laboratory simulations may contribute to these scientific efforts.

Microwave-heating techniques used in industrial and domestic applications have a unique feature of inner-body heating. Unlike convective heating, the microwave energy is transmitted electromagnetically into the body, and is converted to heat inside. A hotspot effect (undesired in most other microwave applications) may evolve due to the thermal-runaway instability [3].

Basalt microwave-heating experiments were presented in various aspects. Melting of basalts in a microwave cavity was introduced in 2004 [4]. More recently, microwave heating of basalt at lower temperatures was studied in various conditions in [5]. The formation of cracks due to temperature gradients and thermal stresses was analyzed by a thermo-mechanical model [6]. Larger basalt stones, of $\sim 400 \text{ cm}^3$, were heated by microwaves to $\sim 500^\circ\text{C}$ in their core [7].

Here we study basalt melting and demonstrate volcano-like effects in a $\sim 3\text{-cm}$ scale, as in [4]. This laboratory setup, regarded as a *microwave-induced miniature-volcano* demonstrator, exhibits hotspots, volcanic-like bursts and eruptions, solidification of lava flows to black glass, etc., similarly to real volcanic phenomena. The numerical model [8], in agreement with the experimental results, reveals the thermal-runaway instability at the initial melting as the main cause for the heat concentration in the core of the basalt stone, and as the generator of the various volcanic-like effects observed in this experiment.

MATERIALS AND METHODS

Dry basalts are electrical insulators at room temperature, but their resistivity decreases exponentially as the temperature grows. Near melting temperatures ($\sim 1,085^\circ\text{C}$) they become electrical conductors. The thermal conductivity of basalt decreases as the temperature increases (unlike volcanic glass which has a minimum at $\sim 700^\circ\text{C}$). These properties [9-13], listed in Table 1 make the basalt a good candidate for microwave-heating in a thermal-runaway process, as performed in this experiment in order to create a hotspot in the core of such stone.

The experimental setup includes a cavity (made of a WR-340 waveguide) fed by a 2.45 GHz, 0.9 kW magnetron as shown in Fig. 1. A basalt stone, either in its natural form or cut as a cubic brick of 3 cm length, is placed inside the cavity in an optimized position. The visual observation of the heating is enabled by the microwave-cutoff vanes along the waveguide as established by video and thermal camera (FLIR-SC300). The incident and reflected waves are recorded by an impedance analyzer (Homer, S-Team Ltd.). An optical spectrometer (Avantes, Avaspec-3648) in the 200-1000 nm range with 0.3 nm spectral resolution is used to capture the emitted light from the lava eruption.

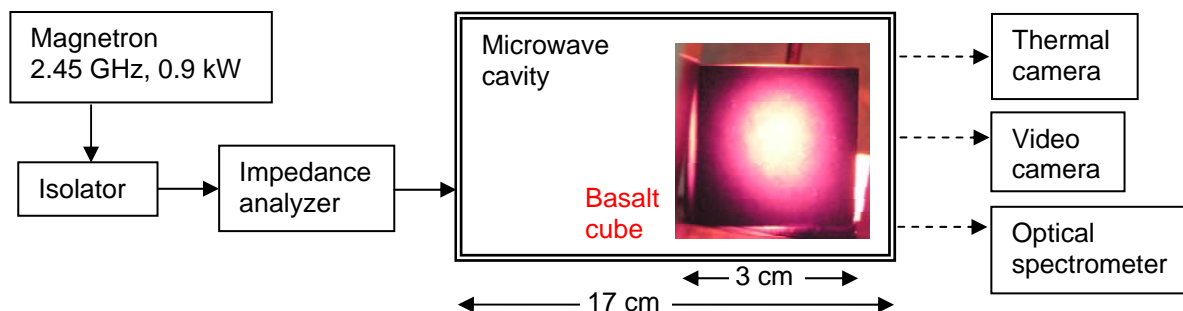


Figure 1. The experimental setup for basalt melting with a 3-cm cubic brick molten inside.

The heating process is modelled by solving the coupled electromagnetic-thermal equations [8] in the 3D domain, using COMSOL Multiphysics software and database. The basalt thermal and EM properties, in particular the dielectric permittivity and electrical conductivity, are imported to the model with their temperature dependence as in Table 1. The waveguide walls are modelled as perfect conductors in the boundary conditions for the EM equations. The heat generated within the cubical basalt stone is transferred to the environment by blackbody radiation, by air convection to the surrounding atmosphere, and by heat transfer to the cavity floor at room temperature.

RESULTS AND DISCUSSION

The microwave radiation heats the basalt brick up to its melting temperature. The consequent eruption of lava which originates from the cube's core outwards is clearly observed in Figs. 2a,b and Figs. 2c,d, for a cubic brick and a natural stone, respectively. The thermal images in Figs. 2b and 2d show the molten lava flow from the core outwards in both cases.

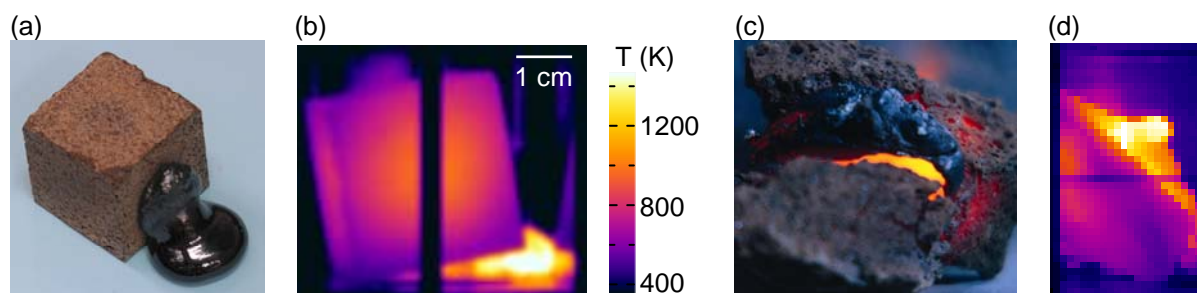


Figure 2. Stills and thermal images of a basalt brick (a, b) and a natural stone (c, d) molten inside. The images after (a) and during (c) the irradiation show the lava flow and its solidification to a black glass (obsidian). The thermal images (b, d) show the lava eruption from the inside out through cracks created due to the heating.

The surface temperature which evolves on the outer brick face is captured by the thermal camera, and compared to the theoretical model as presented in Figs. 3a, b. Figure 3a shows the temperature evolution accumulated in 5 runs in the same experimental conditions compared to theory. The inset shows a colour map of the spatial temperature measured by the thermal camera. The spatial temperature profile evolution is presented in Fig. 3b as measured along the height dimension of the face, and compared to the numerical simulation in various times ($t = 0.5, 1, 2 \dots 8$ min). A reasonable agreement is noticed between experiments and theory.

Table 1. Temperature-dependent basalt's properties [9-13] used in the numerical simulation. The melting temperature is $T_m = 1358$ K and the N -th order polynomial is denoted by $P_N(a_0, a_1, \dots, a_N) = \sum_{n=0}^N a_n T^n$.

| Property | Symbol | Unit | Value / Expression | |
|-----------------------|---------------------------------|----------------------------------|---|---|
| | | | $T < T_m$ | $T_m \leq T < 1,600$ K |
| Relative Permittivity | $\varepsilon' - j\varepsilon''$ | | $8.18 - j0.708$ | $5.95 - j0.208$ |
| Mass density | ρ | kg m^{-3} | 2670 | 2650 |
| Specific heat | C_p | $\text{J kg}^{-1} \text{K}^{-1}$ | $P_4(-217.4, 6.4, -0.012, 10^{-5}, -3.1 \cdot 10^{-9})$ | $P_3(250.22, 2.56, -0.003, 1.26 \cdot 10^{-6})$ |
| Thermal conduction | K | $\text{W m}^{-1} \text{K}^{-1}$ | $P_4(3.71, -0.0026, -9.03 \cdot 10^{-6}, 1.47 \cdot 10^{-8}, -5.78 \cdot 10^{-12})$ | $P_2(0.13, 0.0028, -1.65 \cdot 10^{-6})$ |
| Electric conductivity | $\sigma(T)$ | $\Omega^{-1} \text{m}^{-1}$ | $110 \cdot \exp(-12,093T^{-1})$ | $3.8 \cdot 10^5 \exp(-16,977T^{-1})$ |
| Emissivity | ε | | 0.74 | |

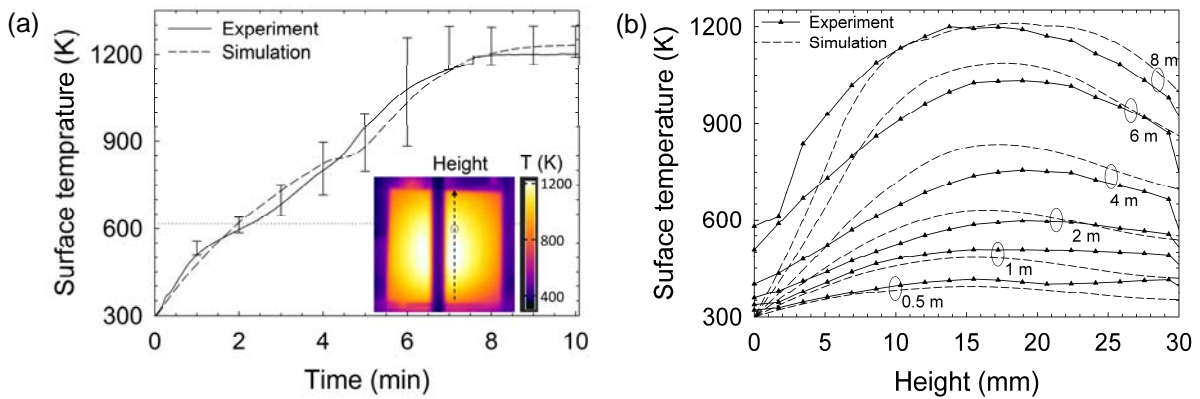


Figure 3. Temporal (a) and spatial (b) temperature evolution on the cubic brick surface, in a comparison of experimental (solid line) and theoretical (dashed line) results.

The optical spectrum of the emitted light from the molten basalt, presented in Fig. 4a, provides an additional means to estimate the surface temperature (note that Wien's displacement law is not applicable in this range). Planck's law is used for this purpose in the form $\lambda \ln(I\lambda^5) = \lambda A - hc/kT$ where λ , h , c , and k are the optical wavelength, the Planck's constant, the speed of light, and the Boltzmann constant, respectively, and the relative value of A varies with the intensity of the light emitted. The intensity fit shown in Fig. 4a yields 1,399 K, slightly higher than the melting temperature, with $R^2=0.9997$. The microwave reflection coefficient measured in 5 typical runs is shown in Fig. 4b in a comparison with the theoretical simulation result. The sudden drop of the microwave reflection, from ~ 0.8 to ~ 0.4 , coincides with the thermal-runaway instability and the initial melting effect (note the simulated core temperature in Fig. 4b). The former variation of the reflection from ~ 0.5 to ~ 0.8 , which is not seen in the simulation, might be a result of humidity within the basalt that evaporates during the initial heating stage.

CONCLUSIONS

The feasibility of basalt melting by localized microwaves is demonstrated here, following [1, 4]. The thermal-runaway instability seems most significant at the initial melting moment, associated with a relatively large drop in the microwave reflection as observed in Fig. 4b. This effect is attributed to the (almost two orders of magnitude) difference between the effective electrical conductivity of basalts in solid and liquid (lava) states. This transition leads to the sudden rise in the core temperature, due to

the thermal-runaway instability in the "seed" location (where the initial phase transition occurs). This may explain the significant difference in temperatures between the inner core of the stone and its outer surface. This temperature gradient might lead to thermal stresses which eventually lead to crack formation, as observed. A further investigation of this effect requires a specific equation of state for basalt. Yet, a good agreement is noted between the experimental and theoretical results. This agreement validates both the numerical model and the basalt's temperature-dependent properties used.

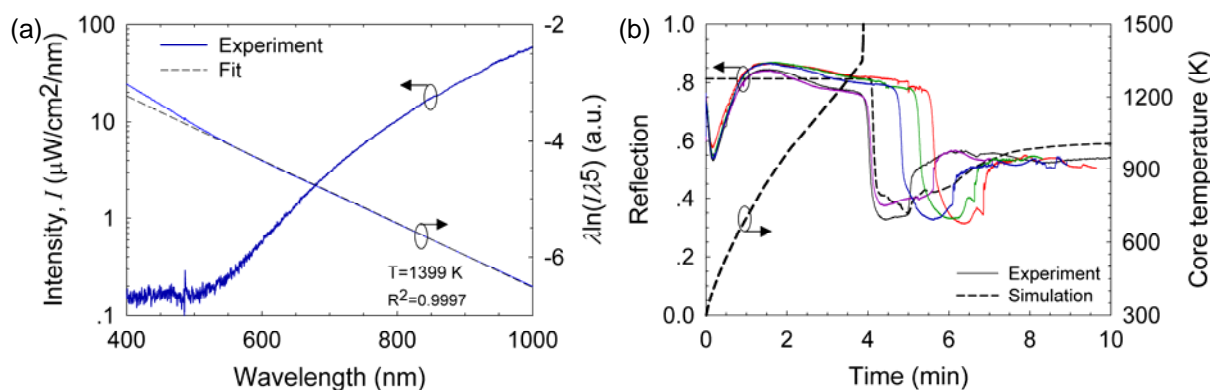


Figure 4. (a) The optical spectrum emitted from molten basalt and its blackbody radiation fit, yielding 1,399 K. (b) The reflection coefficient, measured and simulated, during the heating, and the simulated core temperature.

The ability to melt basalts by localized microwaves, such as provided by the microwave drill [2], can be utilized in a variety of practical applications, e.g. in construction, drilling, joining, mining and fracturing operations. In addition, the resemblance to volcanic effects demonstrated by the microwave setup may facilitate means for new scientific experiments, laboratory simulations, and educational demonstrations of volcanic effects and related geophysical phenomena.

ACKNOWLEDGEMENTS

This research was supported in part by the Israel Science Foundation under Grant No. 1639/11.

REFERENCES

- [1] Decker R., Decker B., *Volcanoes*, 3rd ed (Freeman, New York, 1998).
- [2] Jerby E., Dikhtyar V., Aktushev O., Groslick U., The Microwave Drill *Science* **298**, pp. 587-589, 2002.
- [3] Parris P.E., Kenkre V.M. Thermal runaway in ceramics arising from the temperature dependence of the thermal conductivity. *physica status solidi (b)* **200**, pp. 39-47, 1997.
- [4] Jerby E., Dikhtyar V., Einat M., Microwave melting and drilling of basalt *AICHE Annual Meeting, Nov. 7-12, 2004, Austin, Texas, Proc.*, p. 1673, 2004 (Publisher: American Institute of Chemical Engineers).
- [5] Peinsitt T., Kuchar F., Hartlieb P., Moser P., Hubert Kargl, Restner U. and Sifferlinger N. A., Microwave heating of dry and water saturated basalt, granite and sandstone *Int. J. Mining and Mineral Engineering* **2**, pp. 18-29, 2010.
- [6] Hartlieb P., Leind M., Kuchar F., Antretter T. and Moser P., Damage of basalt induced by microwave irradiation *Minerals Eng.* **31**, pp. 82-89, 2012.
- [7] Mamontov A. V., Nefedov V. N., Tuv A. L. Yazykov D. A., An investigation of the possibility of melting basalt using microwave energy *Meas. Tech.* **55** (9), pp. 1068-1070, 2012.
- [8] Jerby E., Aktushev O. and Dikhtyar V., Theoretical analysis of the microwave-drill near-field localized heating effect *J. Appl. Phys.* **97** (3) 034909, 2005.
- [9] Presnall, D.C., Simmons C.L., & Porath H. Changes in electrical conductivity of synthetic basalt during melting *J. Geophys. Res.* **77**, 5665-5672 (1972).
- [10] Frasci L.L., McLean, S.J., Olsen, R.G. Electromagnetic properties of dry and water saturated basalt rock, 1-110 GHz. *IEEE Trans. Geoscience and Remote Sensing* **36**, 754-766 (1998).
- [11] Sahagian, D.L., Proussevitch A.A., Carlson W.D., Analysis of vesicular basalts and lava emplacement processes for application as a paleobarometer/paleoaltimeter *Jour. Geology* **110**, pp. 671-685, 2002.
- [12] Burgi P., Caillet M., Haefeli S., Temperature measurements at Erta' Alel lava lake, Ethiopia Société de Volcanologie Genève, C.P 6423,1211, Geneva 6, Switzerland, pp. 472-485, 2002.
- [13] Carter L.M, Campbell B., Holt J., Phillips R., Putzig N., Mattei S., Seu R., Okubo C., Egan A., Dielectric properties of lava flows west of Ascraeus, Mons, Mars, *Geophysical Res. Letters* **36**, pp 1-5, 2009.